



HAL
open science

Adaptive Sampling for Fast and Accurate Metamodel-Based Sensitivity Analysis of Complex Electromagnetic Problems

Paul Lagouanelle, Fabio Freschi, Lionel Pichon

► **To cite this version:**

Paul Lagouanelle, Fabio Freschi, Lionel Pichon. Adaptive Sampling for Fast and Accurate Metamodel-Based Sensitivity Analysis of Complex Electromagnetic Problems. *IEEE Transactions on Electromagnetic Compatibility*, 2023, 65 (6), pp.1820-1828. 10.1109/TEMPC.2023.3320285 . hal-04242561

HAL Id: hal-04242561

<https://hal.science/hal-04242561>

Submitted on 15 Oct 2023

HAL is a multi-disciplinary open access archive for the deposit and dissemination of scientific research documents, whether they are published or not. The documents may come from teaching and research institutions in France or abroad, or from public or private research centers.

L'archive ouverte pluridisciplinaire **HAL**, est destinée au dépôt et à la diffusion de documents scientifiques de niveau recherche, publiés ou non, émanant des établissements d'enseignement et de recherche français ou étrangers, des laboratoires publics ou privés.

Adaptive sampling for fast and accurate metamodel-based sensitivity analysis of complex electromagnetic problems

Paul Lagouanelle^{*†}, Fabio Freschi^{*}, Lionel Pichon[†]

^{*} Dipartimento Energia “G. Ferraris”, Politecnico di Torino, 10129 Torino, Italy

[†] GeePs – Group of electrical engineering - Paris, UMR CNRS 8507, CentraleSupélec, Université Paris-Saclay Sorbonne Université, 3 & 11 rue Joliot-Curie, Plateau de Moulon 91192 Gif-sur-Yvette, France

Abstract—This paper presents the development of an adaptive sampling strategy for building surrogate models of complex electromagnetic (EM) systems. Accurate sensitivity analysis is crucial to electromagnetic compatibility (EMC) but usually requires a few thousand calls of the numerical model if performed using classical Monte-Carlo sampling. In the case of an expensive computational model, this results in extremely long computation. Hence why, with only a few calls of the numerical model, surrogate models are built to approximate the behavior of the system. This accurate predictor can then be used instead of the expensive computational model for various analysis. The active learning sampling strategy has been tested successfully on a realistic finite element method (FEM) model.

Index Terms—Numerical models, approximation methods, metamodeling, sensitivity analysis.

I. INTRODUCTION

Sensitivity analysis (SA) can be used on both numerical models and experimental prototypes in order to predict and quantify the variations of an output of interest regarding defined variations of input parameters. Thus, helping in the design of new systems and the improvement of existing devices. Due to the recent growth of electrical engineering for both domestic and industrial applications, the need of fast and accurate sensitivity analysis for such complex systems has been constantly increasing in the case of EMC engineering.

Because of the overall complexity of most current numerical models, computation time is increasing rapidly for sensitivity analysis when the variation of several input parameters at once is considered. A possible work-around is to use surrogate modeling (or metamodeling), which builds a predictor of the model using a given training dataset. This metamodel is an analytical function which can be computed fastly a great number of times. It can be used in lieu and place of the existing simulation model (or experimental model). Thus, the global sensitivity analysis, like Sobol’ indices [1] computed with Monte-Carlo methods, is performed on the predictor at a low computation cost easily.

Thanks to their flexibility: easy to implement, great efficiency with stochastic models, high accuracy for high-order interaction and non-linearities, metamodels enables fast and easy computation of global sensitivity indices on complex numerical models [2], providing an accurate metamodel has been built. Regarding EMC problems in general, many

numerical methods have been recently developed in order to reduce the numerical cost of sensitivity analysis. In [3], both Response Surface Methodology (RSM) and Polynomial Chaos expansion (PCE) are used to perform accurate sensitivity analysis of crosstalks among differential vias. Both methods have been successfully validated using simulations data. As in [4], where PCE has been used successfully to construct a surrogate model of the radiated field in shielded wires. Surrogate models can also be used for optimization in EMC design, as in [5], where an RSM-based optimization process is used to efficiently design multilayered shields.

The goal of the work presented here is to reduce the number of samples needed for the surrogate model setup, thus, reducing the number of calls of the heavy computational model. In [6], a performance-driven modeling is fully developed and validated for the design of antenna structures. Koziel and Pietrenko-Dabrowska managed to reduce the number of calls of the EM model by 60% (on average) compared to a classical analysis. In [7], the use of Smolyak’s sparse grid algorithm is presented for uncertainty quantification for EM systems. As in [7], most of these numerical methods can be enhanced using adaptive sampling to greatly reduce the initial samples for the metamodel setup [8]. In [9], radiated immunity test are studied with a Thévenin-based metamodel paired with a simple adaptive sampling, which manages to reduce the computation time from ~ 119 h using a FEM solver to only 19 s. For complex EMC problems, adaptive sampling has notably been used with Kriging metamodeling of radiated susceptibility in coaxial shielded cables [10]. But also to perform global sensitivity analysis of an electromagnetic interference filter [11].

Therefore, this work focuses on the design of an adaptive sampling strategy for metamodeling. Firstly, this paper presents the development and the design parameters required for an adaptive strategy for PCK metamodeling. Then, based on various test functions and several sampling strategies, a partition design is selected to greatly reduce the number of calls of the input computational model. The core of the work lies in the careful selection of the refinement design, where the parameter space is subdivided based on a local non-intrusive cross-validation (CV) criterion. Unlike other existing adaptive strategies, the global consistency of the metamodel is achieved by insuring a local consistency of every surrogate model built

in every partition of the parameter space. Finally, the resulting algorithm is tried on a realistic wireless power transfer (WPT) system FEM model, on which accurate sensitivity analysis are crucial for EMC studies.

II. SURROGATE MODELING ALGORITHM

A. Surrogate model

This work focuses on two surrogate models, PCE and Kriging, along with their combination Polynomial-Chaos-based Kriging (PCK), which have been proven quite efficient for building accurate predictors and performing various global SA on a wide range of complex models. For example in the case of electromagnetic device optimization [12] where Kriging has been proven better compared to other surrogate processes. Polynomial Chaos expansion has been proven successful at approximating Magnetic Flux density at a lower computation cost than regular simulations [13]. As for PCK metamodeling, it has been recently used in the case of computational dosimetry for estimating specific absorption rate values [14].

The surrogate model used here is an exact interpolator: PCK metamodeling combines both PCE and Kriging to predict the variations of a given model $\mathcal{M}(X)$. Kriging is used to interpolate the local variations of the output model while PCE is useful for the global approximation. A PCK metamodel is defined by [15]:

$$\widehat{\mathcal{M}}(X) = \sum_{\alpha \in \mathcal{A}} y_{\alpha} \psi_{\alpha}(X) + \sigma^2 Z(X, \omega) \quad (1)$$

where $\sum_{\alpha \in \mathcal{A}} y_{\alpha} \psi_{\alpha}(X)$ is a weighted sum of orthonormal polynomials describing the trend of the PCK model and $\sigma^2 Z(X, \omega)$ is a zero-mean stationary Gaussian process with a variance of σ^2 . PCK can be interpreted as a Kriging metamodel with a polynomial trend, whose characteristics are unknown. Therefore the PCK metamodel is built in two parts: the computation of the polynomial coefficients (y_{α}) on one side and the kriging hyperparameters on the other side. The computation of these metamodel parameters is performed by the UQLab framework available on Matlab [16].

Let's consider a set $\{(X_1, Y_1), \dots, (X_N, Y_N)\}$ of N input samples. Using this set, one can build a PCK metamodel $\widehat{\mathcal{M}}$. The consistency of the metamodel is evaluated by the Leave-one-out error (LOO):

$$LOO = \frac{1}{N} \sum_{i=1}^N \left(\frac{\|\widehat{\mathcal{M}}_{/i}(X_i) - Y_i\|}{\|Y_i\|} \right)^2 \quad (2)$$

where $\widehat{\mathcal{M}}_{/i}$ is the mean predictor that was trained using all (X, Y) but (X_i, Y_i) . The LOO enables us to evaluate the consistency of the metamodel considering its build. If the LOO is close to 1, the metamodel is highly modified if one datapoint is taken out of the training dataset, whereas the smallest it is, the least it will be modified.

B. Variance-based sensitivity analysis

In order to perform global SA using metamodels, the well-known Sobol' indices [1] have been chosen as our

sensitivity trackers. The first order Sobol' index for a parameter P is a simple quantity varying from 0 (almost independent) to 1 (the more dependent) quantifying the dependency of the output model on a given parameter P regarding a variation of several parameters simultaneously. When using PCE-based metamodels, the computation of the Sobol' indices can be easily extracted from the polynomial decomposition (see equation 1).

Let us consider a model output $\mathbf{Y} = \mathcal{M}(\mathbf{X})$ with d input parameters (P_1, \dots, P_d) . Thanks to the uniqueness of Sobol' decomposition, the output variance $\text{Var}(\mathbf{Y})$ can be expressed as:

$$\begin{aligned} \text{Var}(\mathbf{Y}) &= \sum_{s=1}^d \sum_{i_1 < \dots < i_s} V_{i_1, \dots, i_s} \\ \text{Var}(\mathbf{Y}) &= \sum_{i=1}^d V_i + \sum_{(i,j), i < j} V_{ij} + \dots + V_{12\dots d} \end{aligned} \quad (3)$$

with the following definitions for the partial variance terms:

$$\begin{aligned} V_i &= \text{Var}_{P_i}(\mathbb{E}_{\mathbf{X}_{/i}}(\mathbf{Y}|P_i)) \\ V_{ij} &= \text{Var}_{P_i, P_j}(\mathbb{E}_{\mathbf{X}_{/ij}}(\mathbf{Y}|P_i, P_j)) \\ V_{i_1, \dots, i_s} &= \text{Var}_{P_{i_1} \dots P_{i_s}}(\mathbb{E}_{\mathbf{X}_{/i_1 \dots i_s}}(\mathbf{Y}|P_{i_1}, \dots, P_{i_s})) \end{aligned} \quad (4)$$

The variance can be decomposed in a sum of variance-based terms showing the dependency on each input individually (the V_i in equation 3) but also the second-order (V_{ij}) and higher-order interactions between the various input parameters.

1) *Sobol' indices*: Using the variance decomposition in equation 3, a sensitivity tracker S_u can be defined for any combination of any order of input parameters, $\forall \mathbf{u} = (i_1, \dots, i_s) \in \llbracket 1, d \rrbracket^s, i_1 < \dots < i_s$:

$$S_{i_1, \dots, i_s} = \frac{V_{i_1, \dots, i_s}}{\text{Var}(\mathbf{Y})} \quad (5)$$

The most commonly used Sobol' indices is the first order Sobol' index, $\forall i \in \llbracket 1, d \rrbracket$:

$$S_i = \frac{V_i}{\text{Var}(\mathbf{Y})} = \frac{\text{Var}_{P_i}(\mathbb{E}_{\mathbf{X}_{/i}}(\mathbf{Y}|X_i))}{\text{Var}(\mathbf{Y})} \quad (6)$$

which emphasizes the impact of the parameter P_i alone on the output model compared to other parameters. The closer it is to one, the bigger impact it produces on the model. Higher-order Sobol' indices can be interpreted in the same way, as the sensitivity of the output model is observed regarding the variations of several input parameters simultaneously, the effect each input cannot be separated from the others. The total sum of all orders Sobol' indices verifies:

$$\sum_{i=1}^d S_i + \sum_{(i,j), i < j} S_{ij} + \dots + S_{12\dots d} = \sum_{\{\mathbf{u}, \mathbf{u} \subseteq \llbracket 1, d \rrbracket\}} S_{\mathbf{u}} = 1 \quad (7)$$

2) *Total indices*: For high dimensional output models, the observation of all orders Sobol' indices can be difficult due to the high number of combination. Therefore, for an input parameter P_i , a total-effect index (or total Sobol' index) S_i^T is defined by summing all the Sobol' indices using this variable:

$$S_i^T = \sum_{\{\mathbf{u}, \mathbf{u} \subseteq \llbracket 1, d \rrbracket \text{ and } i \in \mathbf{u}\}} S_{\mathbf{u}} \quad (8)$$

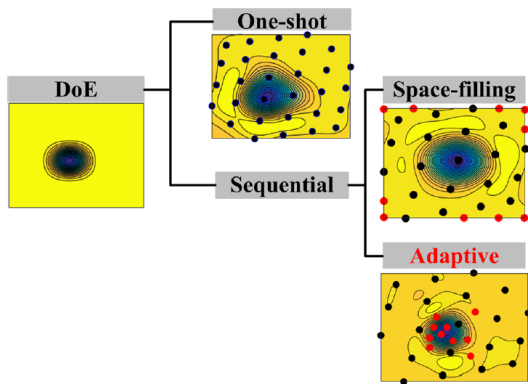


Fig. 1: Visual representation of different sampling strategies, taken from [8]

Unlike S_i where according to equation 7: $\sum_{i=1}^d S_i \leq 1$, this time the sum of all the total Sobol' indices is greater than one:

$$\sum_{i=1}^d S_i^T \geq 1 \quad (9)$$

Indeed, for example for a given couple (P_i, P_j) of input parameters, S_{ij} is counted for both S_i^T and S_j^T . The equality case for inequality 9 is for an output model purely additive. The information given by S_i^T is different from the one given by S_i , for example $S_i \ll 1$ does not imply necessarily $S_i^T \ll 1$. A total Sobol' index close to zero means that the input parameter is almost not affecting the output model, which can be useful for further simulations and experimental designs.

C. Adaptive sampling strategy

Sampling strategies can be classified in two categories: static ("one-shot") sampling and sequential sampling (see figure 1 from [8]). In static sampling, the sample size and the input dataset are chosen prior to the model evaluation. But in our study cases, the input models are rather costly and their response is unknown. Thus, it is hard to determine an a priori sample which would result in a consistent surrogate model. Hence why, sequential sampling methods have been developed, where the input dataset is modified based on previous computations along the build of the metamodel.

Among sequential sampling strategies, the goal of an adaptive sampling strategy (also called active learning) is to start from a rather low number of samples and expand it in the regions of interest of the model response (red samples on figure 1). This results in a relatively low number of calls of the input model compared to space-filling strategies for the same level of surrogate model accuracy.

The general flowchart of an adaptive sampling strategy for surrogate modeling is displayed on figure 2. Given an input parameter space \mathcal{X} for an expensive computational model \mathcal{M} , N samples are drawn from it $\mathbf{X} = (X_1, \dots, X_N)$. Their corresponding model responses are computed $\mathbf{Y} = (Y_1, \dots, Y_N)$ and a first metamodel $\widehat{\mathcal{M}}$ is computed using this

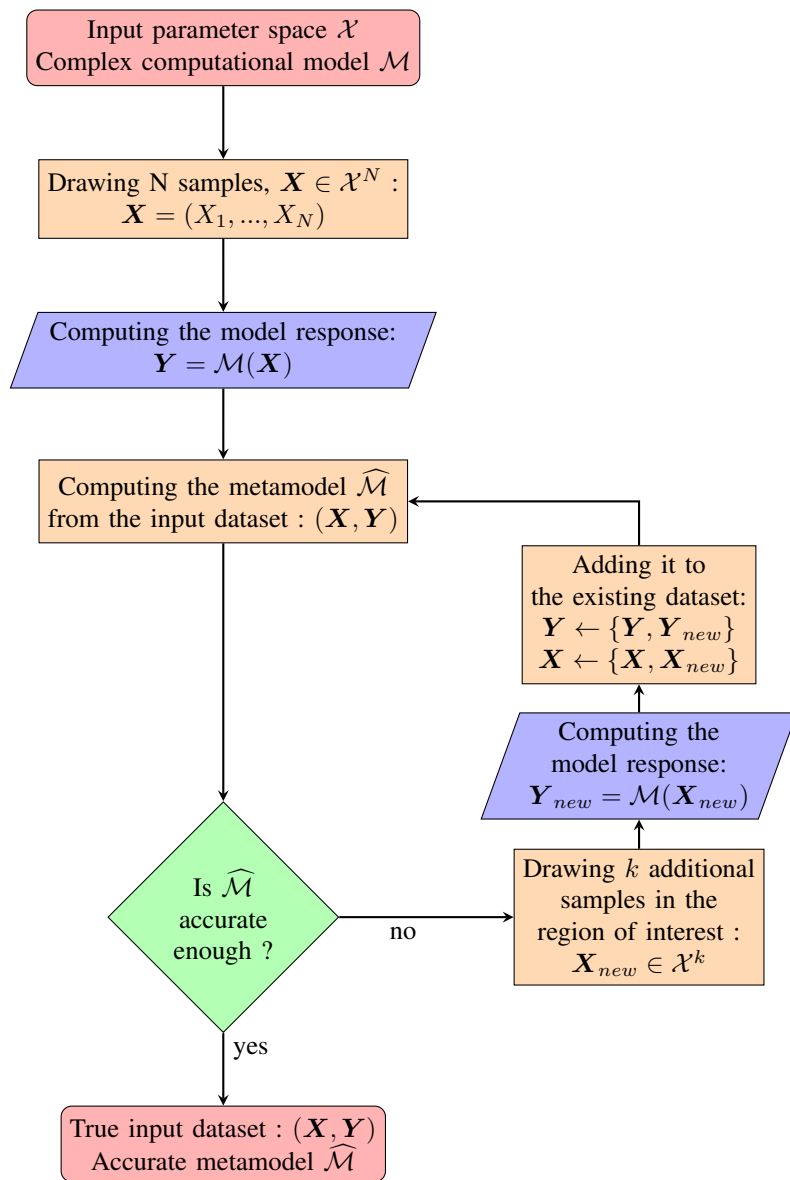


Fig. 2: Flowchart of an active learning metamodeling process, with the blue processes being the computationally expensive steps

dataset. If such a metamodel is not accurate, new samples (along with their responses) are drawn in the regions of interest and the input dataset is enriched. The algorithm stops when the metamodel is accurate enough.

Therefore, for the design of such an active learning metamodeling process, several design parameters need to be explored: a local criterion to expand or not the dataset, a global stopping criterion, the sampling method and finally the definition of the area of interests. The general goal is to minimize the calls of the expensive model function (blue processes in the flowchart).

D. Design parameters

1) *Local criterion*: Most adaptive sampling strategy starts with a space-filling sampling method to explore the input

parameter space as much as possible. Then, the expansion of the dataset in a local area is ruled by the observation of certain local metric. The metric can be model-dependent (variance-based, gradient-based...) which often leads to additional model calls and thus longer computation time in our case, or independent (usually cross-validation errors) using only the existing dataset or the metamodel, which can be computed rapidly using the analytical predictor. Therefore, considering low input dimensionalities (no greater than ten input parameters) for the input parameter space, the aforementioned *LOO* has been considered for the local accuracy of our metamodel (see equation 2). This enables to minimize the call of the computational model.

If the local *LOO* is too high in an area, more samples are needed in this part of the input parameter space. This brings the difficult choice of defining a proper threshold for the *LOO* as a local stopping criterion (see a discussion in [17]). The choice of the *LOO* as a local stopping criteria is highly motivated by its crucial use for existing learning algorithms. Overall, the *LOO* CV error is successful at estimating the consistency of any metamodel while not being the best in every case [18]. Moreover, within a region of interest, the use of *LOO* instead of other k-fold cross-validation error is obvious due to the low number of datapoints considered. Choosing the *LOO* as a local metric ensures that, in every area of interest considered within the input parameter space, the resulting metamodel is locally consistent. Therefore, the metamodel is globally consistent regarding the entire input parameter space.

2) *Partition algorithm*: The choice of a CV-based adaptive sampling leads to an obvious partition design for the area of interests. The main idea is to split each inaccurate region into 2^d sub-regions with d being the dimension of the input space. This quad-tree partition design [19] has already been successfully developed for solving Navier–Stokes equations in aeronautic design [20]. Although this subgridding technique is quite easy to set up, the main drawback of using it is the obvious curse of dimensionality, where the number of computed datapoints would explode for high-dimensional models. Hence why the application of this algorithm and the models studied here have responses only depending on a small number of parameters. Performing global sensitivity analysis prior to a complete active learning algorithm can greatly reduced the number of relevant parameters for a single analysis, thus preventing us from computing too many useless datapoints.

3) *Subdivision limitation*: Usually a trade-off between the local and global criteria needs to be defined, with proper weights given to each metric in order to subdivide or not the current domain. But in order to tackle the curse of dimensionality which appears due to the two previous choices, an obvious choice for the global criterion is to set the maximum number of divisions allowed for the partitioning to limit the total number of computations.

III. COMPARISON OF SAMPLING METHODS

A local and a global stopping criterion have been chosen with the CV *LOO* and a limit for the number of divisions,

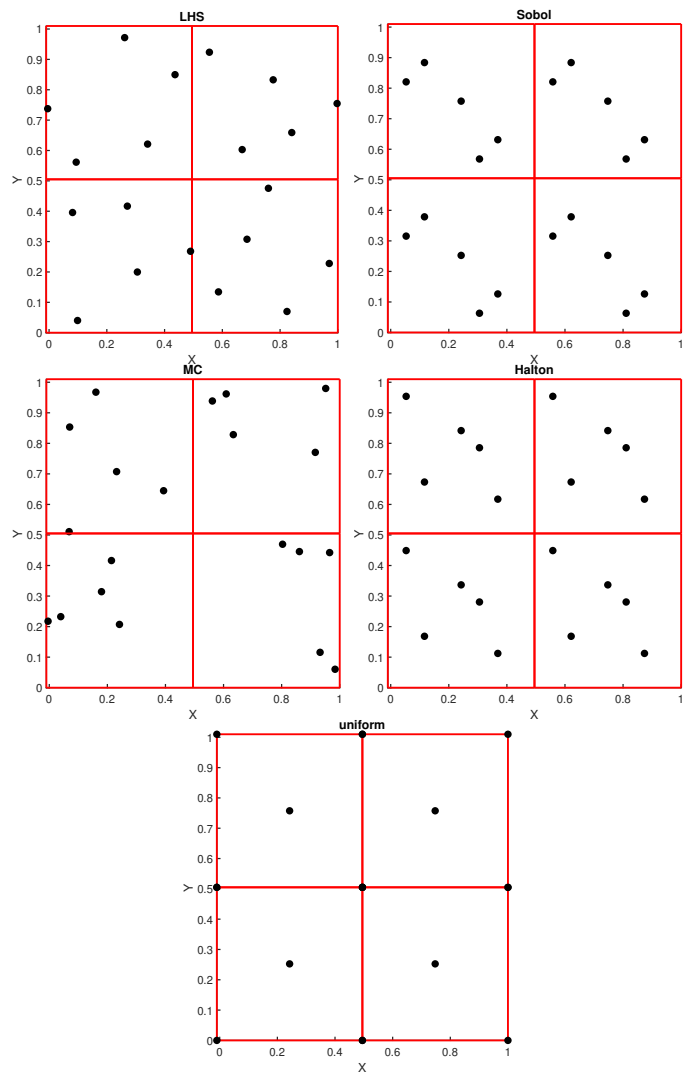


Fig. 3: Sampling methods considered: 20 calls for LHS, Sobol', MC and Halton samplings instead of 12 calls for the uniform sampling for a bidimensional input space

along with a partitioning subgridding technique for the generation of sub-spaces within area of interests where the new samples will be drawn from.

A. Sampling methods considered

Then, the goal is to determine the best way to draw samples within subdomains using either stochastic or deterministic methods. The final goal being to not compute a lot of datapoints due to the possible complexity of the considered output model, therefore a great care should be taken in saving as many datapoints as possible when drawing samples on the various domains. The methods used for generating the initial sample and all the following sub-samples have been considered identical. Thus, once a sub-domain is created with the partitioning, the samples are also exploring the whole sub-space. Five different sampling methods have been investigated, which all have already been proven useful in the case of adaptive sampling for surrogate modeling processes

among the literature [8][21]. Three stochastic sampling methods have been studied:

- Latin hypercube sampling (LHS)
- Sobol' sequence sampling (Sobol')
- Monte Carlo sampling (MC)

Along with two deterministic methods:

- Halton sequence sampling (Halton)
- Uniform sampling

An example of some samples for a bidimensional parameter space is displayed on figure 3 after one division of the partitioning algorithm. For a d dimensions parameter space, the number of samples in each subdomain has been set to $2^d + 1$. This embodies, in the case of a uniform quad-tree design, the 2^d corners and the center of the subdomain. This choice has been motivated by various tests notably when comparing the decrease in the local LOO (higher consistency) when adding centers to the subdomains of an existing uniform partition design.

B. Test functions

The algorithm with the 5 aforementioned sampling methods has been tested against several functions with bidimensional inputs that aims to cover a range of possible computational model output for electromagnetic quantities. These test functions have been chosen purely arbitrary and this choice has only been made based on the type of output which had already been studied and the corresponding variations observed. The four bidimensional test functions are displayed on figure 4:

- a function (a) which embodies the computation of the B-field by an infinite wire with the current X and the distance to the wire Y
- a peak function (b) has also been chosen to represent a possible resonance where the whole bidimensional space is giving low values apart from the peak where the output is 10
- a simple square function: $(X, Y) \rightarrow X^2 + Y^2$ (c)
- a bidimensional wave function (d) with a lot of local and global extrema

C. Consistency of the metamodels

Along testing the various sampling methods on these five functions, three different values for both the LOO threshold $\varepsilon = [0.1, 10^{-2}, 10^{-3}]$ and the maximum number of divisions $m = [2, 3, 4]$ have been tried. Therefore 180 metamodels have been computed with our algorithm for all possible combination with 5 samples on each domain. On figure 5, the different number of samples $n_{samples}$ against their corresponding LOO are displayed for every functions and every sampling methods studied. This number is the total number of samples required for the algorithm to converge.

The consistent metamodels for performing accurate sensitivity analysis will be considered only for $LOO < 10^{-2}$. When comparing the results for the different sampling methods it can be seen that using local uniform sampling does not provide the best metamodels considering the LOO consistency. But some LOO values for non-uniform sampling

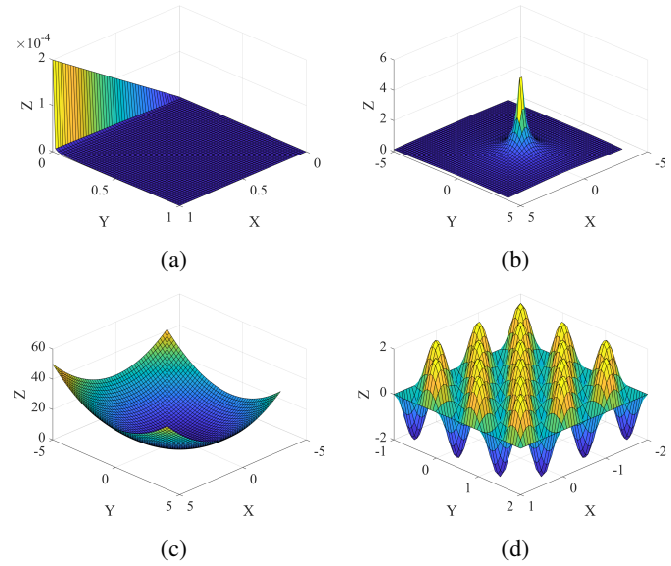


Fig. 4: Test functions for comparing sampling methods on the active learning algorithm

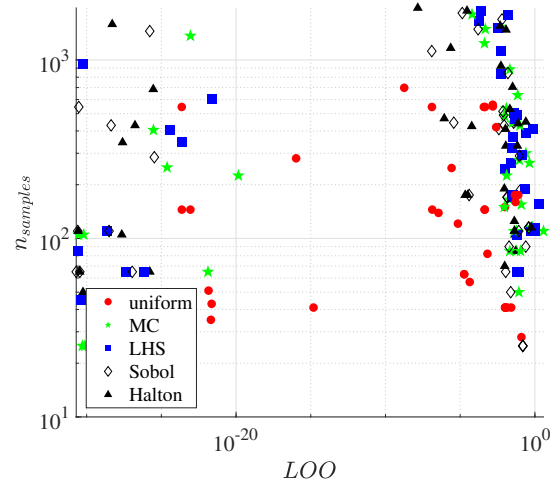


Fig. 5: LOO against $n_{samples}$ for various test cases

are overly small ($< 10^{-20}$), which is not needed and some are using way too many datapoints at the same time. All in all, the uniform sampling is the only one to produce consistent enough metamodels with some decent number of samples which is already too much considering realistic computational model. Considering LOO only, the uniform sampling seems to be the best compromise.

D. Validation tests

But in order to properly assess the accuracy of the predictor at estimating the real model, four MC-generated validation sets of 100 datapoints have been created (one for every test function).

Once a metamodel $\widehat{\mathcal{M}}$ has been computed with a given input dataset, a validation set $\{(X_i, Y_i = \mathcal{M}(X_i)), \forall i \in \llbracket 1, N \rrbracket\}$ can be used to compute a validation error for the metamodel with

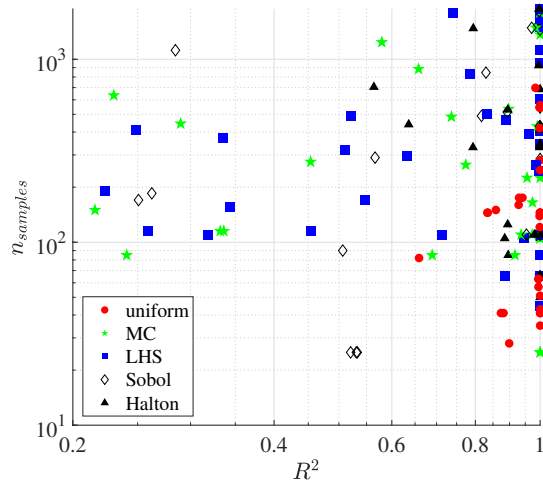


Fig. 6: Validation error R^2 against $n_{samples}$ for various test cases

the well-known coefficient of determination R^2 :

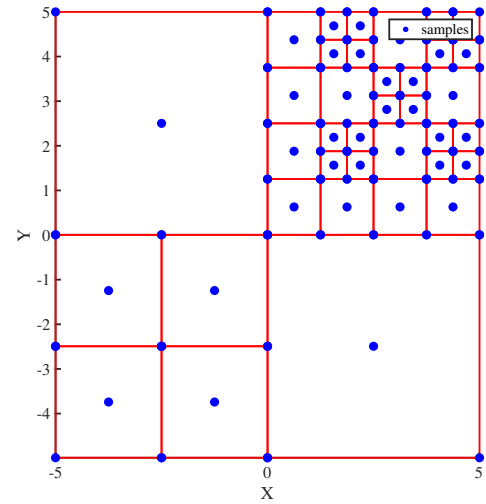
$$R^2 = 1 - \frac{\sum_{i=1}^N \|\widehat{\mathcal{M}}(X_i) - Y_i\|^2}{\sum_{i=1}^N \|\bar{Y} - Y_i\|^2} \quad (10)$$

where \bar{Y} is the mean value of the validation set output. The closer R^2 is to one, the better the predictor is at computing non-sampled datapoints. This coefficient is useful for comparing different metamodels on the same validation set, in order to determine which one gives us the best predictor.

On figure 6, the validation error R^2 has been displayed for the 180 computed metamodels. Among the five considered sampling methods, the uniform sampling is the only one to insure $R^2 \sim 1$ for a fairly low number of samples. For some test cases, MC, LHS, Sobol' and Halton samplings are producing predictors with small coefficient of determination, thus, unable at predicting accurately the behavior of the input model. This makes these four sampling methods highly unreliable for regular use in performing accurate sensitivity analysis using the active learning algorithm. Again, from this second point of view, the uniform sampling is the best sampling method to balance both the number of samples and an accurate enough predictor.

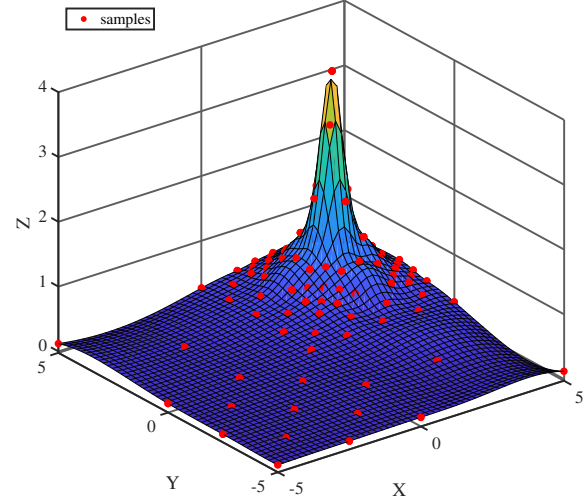
E. Discussion

If another sampling method were to be used for future computations, on these different test functions and for both analysis, Sobol' sequence sampling seems to provide the second best results. When a domain is subdivided into 2^d domains, during the next loop, for the computation of the various metamodels, only 2^d corners needs to be added along with 2^d centers as many datapoints are already available due to previous computations (see a comparison on figure 3). This is the main interest of using a uniform subgridding sampling instead of an LHS or MC sampling which would result on much more datapoints computed. Considering the quad-tree



(a)

PCK metamodel
LOO = 0.06473



(b)

Fig. 7: Results of the active learning algorithm on a peak function (maximum at (3,3)) for $\varepsilon = 0.3$ and $m = 4$: final subdomains and samples (a) and accurate predictor (b) ($n_{samples} = 97$, $LOO \simeq 0.0647$)

partition design with uniform sampling, the maximum number of datapoints computed is:

$$n_{max} = (2^m + 1)^d + 2^{dm} \quad (11)$$

with the number of input parameters d and the maximum number of divisions allowed m .

An example of the final partitioning and predictor for a peak function on a bidimensional input space is shown on figure 7. The resulting predictor needed only 97 datapoints to create a consistent enough metamodel ($LOO \simeq 0.0647$). This shows the great interest of using the quad-tree design coupled with uniform sampling as many datapoints (most of the corners) are within several subdomains which is not the case for other sampling methods. For instance, reproducing the same 50×50 meshgrid without the metamodel predictor would have required 2500 calls of the computational model.

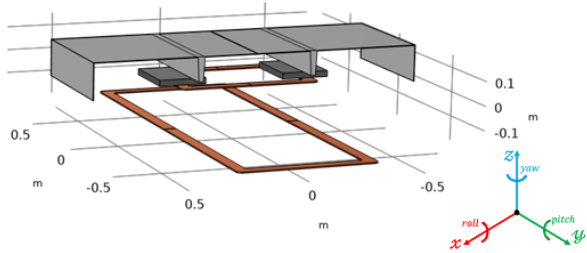


Fig. 8: FEM model for a complete WPT model with 3F3 ferrites cores and an optimized shielding structure

This brings the crucial need to properly tune the LOO threshold ε and the maximum number of divisions m of the active learning algorithm regarding the model behaviour and its dimensionality. As the performance of this algorithm has been fully validated on classical analytical functions, the goal is to extend its application to heavy computational model such as FEM model where the gain in computation time could be of great use.

IV. APPLICATION TO A REALISTIC WPT SYSTEM MODEL

The goal here has been to apply the metamodeling algorithm on a realistic FEM model for a WPT system developed at Politecnico di Torino [22]. Based on this complex model our algorithm tries to build a consistent predictor that can be used for both sensitivity analysis or optimization design in lieu and place of the real model to save computation time.

A. Computational model

Using the CAD model from the WPT system receiver used for experiments at Politecnico di Torino, the complete WPT model has been reproduced with a 3D FEM model displayed on figure 8. For the receiving device, only the main shielding structure optimized with the shielding beams, along with the double U-shaped coils (displayed in orange on figure 8) topped by the 3F3 ferrite cores has been considered. While only the transmitting coil in the ground has been modeled for the transmitter.

Because this model is fitting a real model available inside the laboratory, the effects of mostly design-based geometrical parameters have been considered:

- Δx , Δy and Δz : the misalignments between the receiving and transmitting coils along the x, y and z axis
- w_{rcoil} , l_{rcoil} , w_{tcoil} , l_{tcoil} : the dimensions of the coils
- α , β , γ : the yaw, pitch and roll of the transmitting coil

The output considered in the following analysis is the coupling factor k of the WPT system:

$$k = \frac{M}{\sqrt{L_R L_T}} \quad (12)$$

with M the mutual inductance of the two coils and (L_R, L_T) their respective self-inductance.

Regarding the computation time, one datapoint takes ~ 1 min to compute on an Intel Core i7-10610U, 1.80 GHz, 8 GB of RAM. If one were to perform some brute-force

TABLE I: Parameters with their corresponding ranges for the analysis of a dynamic WPT system ($LOO \simeq 3.00 \cdot 10^{-2}$, $n_{samples} = 65$)

variable	min	max	description	S^T
Δx	-0.25 m	0.25 m	x misalignment	0.139
Δy	-0.5 m	0.5 m	y misalignment	0.138
Δz	-0.15 m	0.15 m	z misalignment	0.261
α	-10°	10°	yaw	0.136
β	-2°	2°	pitch	$1.97 \cdot 10^{-3}$
γ	-2°	2°	roll	0.634

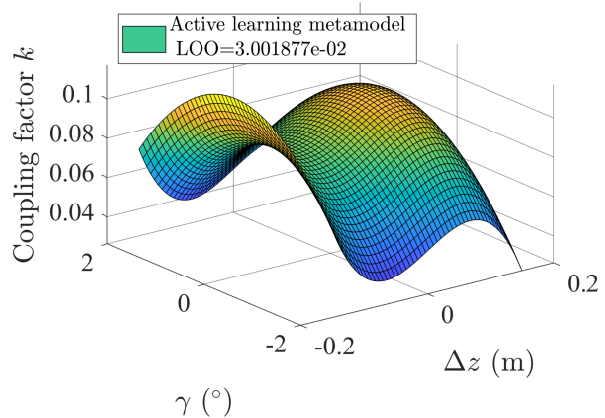


Fig. 9: Variations of the coupling factor k against the z misalignment Δz and the roll γ ($\Delta x = \Delta y = 0$ m and $\alpha = \beta = 0^\circ$)

sensitivity analysis (using Monte Carlo sampling for example), this would require a few thousand calls of the computational model. Thus, the total computation time of the analysis would take several days.

B. Sensitivity to the road profile

The first application has been to compute a consistent predictor for the behavior of the coupling factor regarding the movement of the vehicle and the road profile. The considered parameters for this analysis are displayed in table I. The Δx misalignment and the yaw α have been chosen to consider a car slightly deviating from the center of the road, while the Δy misalignment embodies the direction of motion. The Δz misalignment along with the pitch β and the roll γ take into account the road profile.

The active learning metamodel algorithm managed to build a consistent predictor with $\varepsilon = 0.3$ and $m = 3$. The resulting metamodel uses $n_{samples} = 65$ and has a consistency of $LOO \simeq 3.00 \cdot 10^{-2}$. An example of the variation of the coupling factor produced by the active learning metamodel predictor is displayed on figure 9 for the variations of Δz and γ (a modification of the road profile) with the other parameters set at their nominal values ($\Delta x = \Delta y = 0$ m and $\alpha = \beta = 0^\circ$).

Using this consistent predictor, a sensitivity analysis has been computed using total Sobol' indices displayed on table I. The most important parameters are the roll γ along with the Δz misalignment. As expected these two parameters greatly

TABLE II: Parameters with their corresponding ranges for the analysis of a dynamic WPT system ($LOO \simeq 1.41 \cdot 10^{-2}$, $n_{samples} = 17$)

variable	min	max	description	S^T
w_{rcoil}	0.3 m	0.6 m	receiving coil width	0.105
l_{rcoil}	0.3 m	0.6 m	receiving coil length	0.177
w_{tcoil}	0.3 m	0.6 m	transmitting coil width	0.0614
l_{tcoil}	0.5 m	2 m	transmitting coil length	0.691

increase the distance between the two coils, which decreases significantly the coupling factor. Even if the pitch β also influences the gap between the receiver and the transmitter, for this small range $[-2^\circ, 2^\circ]$ corresponding to an imperceptible bump on the road, its effect is entirely negligible. The roll embodies a non-flatten road which has still a greater impact with such a small range. The other three parameters Δx , Δy and α are taking into account the dynamic aspect for the WPT system and are of course not negligible.

C. Sensitivity to various coil dimensions

Another interesting analysis is to assess the dependency of the coupling factor regarding the transmitter or receiver dimensions. This could emphasize where the greatest care should be taken when designing or building a new WPT system. The considered parameters with their ranges and Sobol' indices are displayed in table II. The algorithm has been ran with $\varepsilon = 0.3$ and $m = 3$ resulting in a metamodel with $LOO \simeq 1.41 \cdot 10^{-2}$ and $n_{samples} = 17$.

The length of the transmitting coil is by far the most important parameter regarding the coupling factor behavior. It ensures the totality of the Magnetic Flux generated is embraced by the receiving coil. Due to the chosen possible dimensions, for the same reason the length of the receiver is also extremely important. As the nominal gap between the coils is $\Delta z = 23.5$ cm, the width of the transmitter has a lesser influence as long as the totality of the Magnetic Flux can be directed to the receiver which is insured with a range $[0.3 \text{ m}, 0.6 \text{ m}]$ similar to the maximum dimensions of the receiver. The receiver dimensions are only limited by the car it can be put in and therefore cannot be extended.

D. Discussion on the algorithm parameters

On table III, the dependency of the maximum number of computed datapoints n_{max} (see equation 11) against the dimension of the input space d and the maximum number of divisions m is displayed for several values. Using the algorithm, if one were to diminish the consistency threshold ε to less than 1% for example, the metamodel for the coil dimensions ($m = 3, d = 4$) would need at the maximum $n_{max} = 10\ 657$, while $n_{max} = 793\ 585$ for the WPT dynamic analysis ($m = 3, d = 6$). Thus, the computation of a metamodel with a higher local consistency would be almost impossible as one datapoint takes ~ 1 min to compute if the resulting sub-metamodels are not consistent.

TABLE III: Maximum number of datapoints n_{max} computed against the dimension of the input space d and the maximum number of divisions m

n_{max}	$m = 0$	$m = 1$	$m = 2$	$m = 3$	$m = 4$
$d = 1$	3	5	9	17	33
$d = 2$	5	13	41	145	545
$d = 3$	9	35	189	1 241	9 009
$d = 4$	17	97	881	10 657	149 057
$d = 5$	33	275	4 149	91 817	2 468 433
$d = 6$	65	793	19 721	793 585	40 914 785

TABLE IV: Computation time of the various steps

Analysis	$n_{samples}$	computation time of all metamodels	computation FEM model	computation sensitivity analysis
road profile	65	~ 1.92 s	1 hour	~ 245 ms
coil dimensions	17	~ 1.55 s	15 min	~ 130 ms

E. Gain in computation time

The goal of the two analyses presented here has been to try our active learning algorithm for accurate sensitivity analysis, in order to save computation time compared to classical methods. When looking at the algorithm flowchart of figure 2, the total computation time for a run of the algorithm needs to consider three different contributions: the calls of the expensive computational model, the computation of the metamodels at every loop and finally the sensitivity analysis.

In table IV, the total computation of time of the various steps of the algorithm are displayed for both analyses. As expected, the only time-consuming step is the call of the FEM model. The computation time of all the metamodels computed in a single run of the algorithm put together does not exceed 2 s for both cases, while the two sensitivity analysis are taking less than 1 s. Therefore the total computation time of the algorithm can be reduced to the calls of the FEM model.

These computation times have been compared to a brute-force analysis where a uniform grid with n_{max} samples have been computed (see equation 11). The results are displayed on table V, the estimated computation time with an extremely refined uniform grid would be in days or even years at six parameters, while our algorithm does not last more than 1 h. Thus, the gain in computation time using this active learning metamodeling algorithm is over 99%. Even if some way better sampling methods (such as MC, LHS, Halton...) could be used in a classical analysis to build the surrogate model, the time reduction compared to a uniform grid would not be greater than 99% [23].

TABLE V: Estimated gain in computation time for the studies on the WPT charger model

Analysis	d	LOO	brute-force analysis (estimated)	adaptive metamodeling algorithm	time reduction
road profile	6	0.030	1.5 year	1 hour	99.99%
coil dimensions	4	0.014	7 days	15 min	99.85%

V. CONCLUSION

Finally, an adaptive sampling algorithm designed for PCK metamodeling of complex electromagnetic problem has been successfully developed. Two analysis on a realistic FEM model have been performed to show the usefulness of such an algorithm. The two computed metamodels have a great consistency ($LOO < 3\%$) which is sufficient for drawing tendencies for sensitivity analysis. The results can be used for future designs or EMC analysis of WPT systems for automotive applications.

As previously developed, the algorithm could show limitations at high dimension input space. An easy solution to this problem is to decrease the number of input parameters by performing factor prioritization. A first wide analysis can be performed on various parameters, giving us a consistent predictor for the model able to perform an accurate sensitivity analysis. Using this sensitivity analysis, only the relevant parameters can be extracted and a finer input space can be chosen with the negligible parameters ignored. Then a better and more consistent metamodel can be built on this smaller set of parameters as it will be able to fully explore the input parameter space thanks to its smaller dimension.

Many improvements for such a numerical method are still possible, but using this algorithm on various FEM models saved more than 99% of computation time compared to classical brute-force analysis. Thus, this method is of great interest for future sensitivity analysis in the case of complex electromagnetic systems.

REFERENCES

- [1] Ilya M Sobol. "Sensitivity analysis for non-linear mathematical models". In: *Mathematical modelling and computational experiment 1* (1993), pp. 407–414.
- [2] Bertrand Iooss and Paul Lemaître. "A review on global sensitivity analysis methods". In: *Uncertainty management in simulation-optimization of complex systems* (2015), pp. 101–122.
- [3] Yansheng Wang et al. "Variability analysis of crosstalk among differential vias using polynomial-chaos and response surface methods". In: *IEEE Transactions on Electromagnetic Compatibility* 59.4 (2017), pp. 1368–1378.
- [4] Kaushik Patra et al. "Surrogate Modeling for Predicting Shielded Cable Emissions". In: *IEEE Transactions on Electromagnetic Compatibility* 65.1 (2022), pp. 249–256.
- [5] Hongcai Chen et al. "Fast design of multilayered shields using surrogate model and space mapping". In: *IEEE Transactions on Electromagnetic Compatibility* 62.3 (2019), pp. 698–706.
- [6] Slawomir Koziel and Anna Pietrenko-Dabrowska. "Knowledge-based performance-driven modeling of antenna structures". In: *Knowledge-Based Systems* 237 (2022), p. 107698.
- [7] Ping Li and Li Jun Jiang. "Uncertainty quantification for electromagnetic systems using ASGC and DGTD method". In: *IEEE Transactions on Electromagnetic Compatibility* 57.4 (2015), pp. 754–763.
- [8] Haitao Liu, Yew-Soon Ong, and Jianfei Cai. "A survey of adaptive sampling for global metamodeling in support of simulation-based complex engineering design". In: *Structural and Multidisciplinary Optimization* 57.1 (2018), pp. 393–416.
- [9] Riccardo Trincherò, Igor S Stievano, and Flavio G Canavero. "Black-box modeling of the maximum currents induced in harnesses during automotive radiated immunity tests". In: *IEEE Transactions on Electromagnetic Compatibility* 62.2 (2019), pp. 627–630.
- [10] Tarek Bdour, Christophe Guiffaut, and Alain Reineix. "Use of adaptive kriging metamodeling in reliability analysis of radiated susceptibility in coaxial shielded cables". In: *IEEE Transactions on Electromagnetic Compatibility* 58.1 (2015), pp. 95–102.
- [11] Arnold Bingler, Sándor Bilicz, and Márk Csörnyei. "Global Sensitivity Analysis Using a Kriging Metamodel for EM Design Problems With Functional Outputs". In: *IEEE Transactions on Magnetics* 58.9 (2022), pp. 1–4. DOI: 10.1109/TMAG.2022.3167105.
- [12] Luiz Lebensztajn et al. "Kriging: A useful tool for electromagnetic device optimization". In: *IEEE Transactions on Magnetics* 40.2 (2004), pp. 1196–1199.
- [13] Peter Offermann and Kay Hameyer. "A polynomial chaos meta-model for non-linear stochastic magnet variations". In: *COMPEL-The international journal for computation and mathematics in electrical and electronic engineering* (2013).
- [14] Pierric Kersaudy et al. "A new surrogate modeling technique combining Kriging and polynomial chaos expansions—Application to uncertainty analysis in computational dosimetry". In: *Journal of Computational Physics* 286 (2015), pp. 103–117.
- [15] Roland Schobi, Bruno Sudret, and Joe Wiart. "Polynomial-chaos-based Kriging". In: *International Journal for Uncertainty Quantification* 5.2 (2015).
- [16] Stefano Marelli and Bruno Sudret. "UQLab: A framework for uncertainty quantification in Matlab". In: *Vulnerability, uncertainty, and risk: quantification, mitigation, and management*. 2014, pp. 2554–2563.
- [17] Ping Jiang et al. "A novel sequential exploration-exploitation sampling strategy for global metamodeling". In: *IFAC-PapersOnLine* 48.28 (2015), pp. 532–537.
- [18] André Elisseeff, Massimiliano Pontil, et al. "Leave-one-out error and stability of learning algorithms with applications". In: *NATO science series sub series iii computer and systems sciences* 190 (2003), pp. 111–130.
- [19] Raphael A Finkel and Jon Louis Bentley. "Quad trees a data structure for retrieval on composite keys". In: *Acta informatica* 4.1 (1974), pp. 1–9.
- [20] Thierry Braconnier et al. "Towards an adaptive POD/SVD surrogate model for aeronautic design". In: *Computers & Fluids* 40.1 (2011), pp. 195–209.
- [21] Thomas J Mackman et al. "Comparison of adaptive sampling methods for generation of surrogate

- aerodynamic models”. In: *AIAA journal* 51.4 (2013), pp. 797–808.
- [22] Vincenzo Cirimele. “Design and Integration of a Dynamic IPT System for Automotive Applications”. 2017SACLS032. PhD thesis. Université Paris-Saclay, Politecnico di Torino, 2017. URL: <http://www.theses.fr/2017SACLS032/document>.
- [23] Chandrika Kamath. “Intelligent sampling for surrogate modeling, hyperparameter optimization, and data analysis”. In: *Machine Learning with Applications* 9 (2022), p. 100373.